Sensors and Actuators B 231 (2016) 659–665

Contents lists available at ScienceDirect

Sensors and Actuators B: Chemical

journal homepage: www.elsevier.com/locate/snb

Cells-on-chip based transducer platform for probing toxicity of metal nanoparticles

Javed H. Niazi[a,*], Ashish Pandey[a,b], Yasar Gurbuz[b], Volkan Ozguz[a], Anjum Qureshi[a,*]

[a] Sabanci University Nanotechnology Research and Application Center, Orta Mahalle, 34956 Tuzla, Istanbul, Turkey
[b] Facutly of Engineering and Natural Science, Sabanci University, Orhanli, 34956 Tuzla, Istanbul, Turkey

ARTICLE INFO

Article history:
Received 24 November 2015
Received in revised form 17 February 2016
Accepted 22 March 2016
Available online 23 March 2016

Keywords:
E. coli
Nanoparticles
Cells-on-chip
Nanotoxicity
Dielectric properties

ABSTRACT

In this work, we developed a cells-on-chip based transducer (CoCT) platform for probing toxicity of silver nanoparticles (Ag NPs) using non-Faradaic electrochemical impedance spectroscopy (nFEIS). This transducing platform was consists of arrays of capacitor on chip in which each capacitor was functionalized with living *Escherichia coli* cells. These cells were capable of responding to exposure of different size and concentration of Ag NPs. The capacitive response of CoCT was dependent on size and concentration of NPs. *E. coli* cells-on-chip response exhibited dramatic loss of capacitance and showed that maximum toxicity to cells-on-chip occurred with smaller 10 nm sized Ag NPs compared to larger size of 100 nm NPs. The cells tend to resist to the larger 100 nm size of NPs that did not affect the cells-on-chip. Our results demonstrated that whole-cell biosensor chip response at a particular frequency enabled determining the severity of the stress imposed by smaller size of Ag NPs. Further, our results were validated through fourier transform infrared spectroscopy (FTIR) and growth of cell/cellular debris and also determined the NPs stress induced toxicity in cells as a proof-of-concept. The methodology developed in this study potentially be extended to other nanomaterials (NMs) for classifying toxic from non-toxic NMs.

© 2016 Elsevier B.V. All rights reserved.

1. Introduction

The nanotechnology industry is rapidly growing with promises of substantial benefits that will have significant economic and scientific impacts. It is also applicable to whole host of areas ranging from aerospace engineering and nano-electronics to environmental remediation and medical healthcare [1]. It is estimated that over 500 consumer goods that are already available consist of variety of nanomaterials (NMs). Nanoparticles (NPs) are present in some sunscreens, cosmetics, toothpastes, sanitary-ware coatings, silicon chips and even in food products. Worldwide investment on nanotechnology is on the rise [2,3] and the trend is expected to continue over the next decade. Unusual physicochemical properties of engineered NMs are attributable to their small size, chemical composition, surface structure, solubility, shape, and aggregation [4]. Yet, concerns have been raised due to the unique properties of nanostructured materials could potentially lead to unforeseen health and environmental hazards. Due to expanding use of NMs and commercialization of nanotechnology products, their exposure in the environment and to humans tend to increase with time. Colloidal silver, including formulations now known to contain silver nanoparticles (Ag NPs), has been used commercially for almost 100 years [5]. However, registration of nanosilver products has increased dramatically over the last decades [5,6], most likely as a result of improved capabilities in nanoscience and engineering that allow Ag NPs to be formulated to confer increased durability and/or sustained antibacterial action, even under harsh environmental conditions [7,8]. As is the case for many other types of nanoparticles, a controversy has arisen about whether the Ag NPs should be subjected to increased regulatory scrutiny compared to macroscale or "bulk" silver. Indeed, Ag NPs have been demonstrated to exhibit toxic effects in plants and bacteria at environmentally relevant concentrations [9]. To date, most traditional biological methods for *in vitro* and *in vivo* toxicological studies of Ag NPs and other engineered NMs on microbial cells are based on cellular activity and proliferations. These methods include growth and viability assays [10–12], proteomic assays, reactive oxygen species (ROS) detection tests [13–15] and molecular-level evaluations based on genetic responses [5,16,17]. Recntly, size dependent effect of Ag NPs against aerobic bacteria *Escherichia coli* and anaerobic oral pathogenic bacteria *Aggregatibacter actinomycetemcomitans*, *Fusobacterium nuceatum*, *Streptococcus mitis*, *Streptococcus mutans and Streptococcus sanguis* have been studied through cell growth

* Corresponding authors.
E-mail addresses: javed@sabanciuniv.edu (J.H. Niazi), anjum@sabanciuniv.edu (A. Qureshi).

http://dx.doi.org/10.1016/j.snb.2016.03.105
0925-4005/© 2016 Elsevier B.V. All rights reserved.

method [18]. Among all of the above methods, *in vitro* cytotoxicity methods are currently employed, which required labeling with fluorescent molecules for detection. These methods are used as markers for cell-viability and consist of procedures that provide results only at a final time-point [19]. The existing conventional analytical techniques reported in the literature usually requires a lengthy and time-consuming process and often produce false positives, and often cannot be implemented for studying cell behavior without interference from its surrounding environment. Hence, there is a demand for a rapid, sensitive and accurate method for assessing toxicity in cells.

Recently, due to the advantages of automation of fluids and minimization of human errors, integration of a cells-on-a-chip system is gaining importance for nanotoxicity assessments [20]. In recent studies, chip-based electrochemical approach was used to test the toxic effect of NMs. The measurements were recorded based on differential pulse voltammetry and or electrical impedance methods [21–23]. All the above cells-on-chip approaches for nanotoxicity assessment were based on Faradaic-electrochemical measurements that require a redox mediator/chemical reagent to generate detectable signal which often leads to undesirable quenching effects with NPs. Therefore, the present study aims to develop toxicity assay using electrical sensing platform that provides a new tool to understand the toxicological impacts of Ag NPs as model for other NMs using bacterial cell-functionalized biosensor chip.

In this study, we designed a CoCT using electrical sensing platform that provides a new tool to understand the toxicological impacts of Ag NPs as model for other NMs. This CoCT measures the capacitance from immobilized cells over electrodes as a function of applied AC frequency and its measuring principle is based on non-faradiac method. Changes in capacitance can be detected that occurred as a result of changes in the cellular activity after their interaction with NPs. The results obtained from the CoCT studies were confirmed through optical imaging, FTIR as well as probing cellular interactions at the cell-membrane after exposure of NPs by growth assay. The fact that the present study is different from the previous reports in an important consideration that include the deleoped biochip was tested for metal oxide NPs and it is important to test metal NPs response as well to extend the applicability of developed CoCT to other NMs [24].

2. Material and methods

2.1. Reagents

Silicon wafers of 4 inch size, (100) oriented, p-type with the resistivity of 9–12 Ω cm and thicknesses of 500 ± 25 μm with 1 μm thick SiO_2 layer on top were obtained from University Wafers, USA. Wild-type *E. coli* DH5α strain was used as model living bacterial cells in this study. Luria-Bertani broth (LB-broth) and Luria-Bertani agar (LB-agar) were obtained from Difco (MI, USA). Phosphate-buffered saline (PBS), 3-mercaptopropionic acid (MPA), 1-ethyl-3-[3-dimethylaminopropyl] carbodiimide hydrochloride (EDC) and *N*-hydroxysuccinimide (NHS), Ag NPs (with sizes of 10, 20 and 100 nm) were purchased from Sigma-Aldrich, Germany. All other reagents used in this study were of analytical grade and filtered through 0.22 μm sterile filters.

2.2. Characterization of Ag NPs

The shape and size of Ag NPs used in this study were characterized using transmission electron microscopy (TEM) technique and dynamic light scattering (DLS,Malvern Zetasizer). For TEM characterization sample preparation, 5% solution of each size of Ag NPs were suspended in aqueous medium and then placed on fromvar coated copper grids. The grids were then allowed to dry at room temperature. The images were captured using 2000 SX JEOL-TEM at 160 kV EHT voltage with a magnification of 250Kx.

2.3. Fabrication of capacitor arrays

Gold interdigitated electrode based capacitor sensor arrays were patterned on SiO_2 surface using image reversal technique. In this process, the metal layers were patterned using the dual tone photoresist AZ5214E. A 2 μm thick AZ5214E photoresist was patterned with the help of a mask for a lift-off process in pure acetone as a solvent. Following this step, a very thin tungsten layer of 50–60 nm size was layered to improve the adhesion of gold on the SiO_2 film by DC sputter deposition and about 200–210 nm thick gold layer was deposited. The dimension of each electrode was 800 μm in length, 40 μm in width with a distance between two electrodes of 40 μm. Each capacitor sensor contained 24-interdigitated gold electrodes within a total area of 3 mm^2.

2.4. Immobilization of E. coli cells on capacitor array chip and exposure of NPs

The bacterial strain used in this study was *E. coli* DH5α. Actively growing *E. coli* cells were inoculated into fresh Luria-Bertani (LB) medium and allowed to grow till mid-logarithmic growth phase. The cells were then harvested by centrifugation at 1000*g* for 3 min and washed thrice with phosphate buffered saline (PBS) pH 7.2, and resuspended in same buffer. The cell concentration was determined by colony counting after serial dilution followed by plating on LB-agar plates. The chip was first rinsed with sterile distilled water and dried with pure nitrogen followed by immersing the chip in 20 mM of mercaptopropionic acid (MPA) and incubated overnight at room temperature. The chips were then incubated with a mixture of 1-ethyl-3-(3-dimethylaminopropyl)-carbodiimide (EDC) and 50 mM of *N*-hydroxysuccinimide (NHS) for 2 h. The chip was then removed, thoroughly washed with distilled water and each capacitor in an array was incubated with 5 μl of bacterial suspension containing 8×10^7 colony forming units (CFU) in PBS solution for 2 h. This sensing area was incubated with a series of Ag NPs concentrations (0.2–2 μg/ml PBS containing 0.01% Tween 20) in 5 μl volumes containing three different sizes 10, 20 and 100 nm, respectively for 2 h at 25 °C. The chip was quickly washed with PBS and dried using nitrogen gas. The dried chips were then subjected dielectric measurements.

2.5. Optical microscopy imaging of immobilized E. coli cells on chip

Optical images of the sensors after immobilization of *E. coli* cells on chip were taken using Carl Zeiss Axio Scope A1 MAT.

2.6. Impedance/capacitance measurement

The impedance/capacitance responses were measured sequentially to ensure that chips remain active after every step that includes; (a) bare capacitor sensor, (b) after *E. coli* immobilization and (c) after NPs exposure. A negative control experiment was conducted using capacitor chip containing heat-killed *E. coli* cells. For this, capacitor chips containing immobilized *E. coli* cells (8×10^7) were subjected to heat treatment in an air-tight pre-heated humid chamber at 95 °C for 5 min followed by quickly freezing at −70 °C for 5 min, and thrice at 25 °C for 15 min. The above treatment process was repeated thrice and finally the capacitive chip was dried under N_2 gas. The capacitance response in between the gold interdigitated electrodes of capacitor sensor surface was measured in the frequency range 50 MHz to 1 GHz using a Network Analyzer (Karl-Suss

PM-5 RF Probe Station and Agilent-8720ES). The Network Analyzer was calibrated using SOLT (short-open-load-through) method. The impedance values were exported to MATLAB® software for the analysis. The absolute capacitance values of triplicate experiments were extracted at an effective frequency (f) range (150–300 MHz) and the standard deviations were shown as errors. The relative capacitance variations were calculated from the data obtained within 150–300 MHz frequency range under standard assay conditions using the following Eq. (1) as described previously [25].

$$\frac{C - C_0}{C_0} \times 100 \quad (1)$$

where C is the actual capacitance after the interaction of each sizes of NPs with *E. coli* cells at a particular concentration and C_0 is the capacitance before interaction.

2.7. FTIR spectra of whole-cell based biosensor chip after exposure of Ag NPs

The immobilization of *E. coli* cells on capacitor chip and effect of different sizes of Ag NPs were confirmed by Fourier transform infrared spectroscopy (FTIR) using Thermo scientific Nicolet™ iS™10 FT-IR Spectrometer.

2.8. Determining the growth curves of bacterial cells exposed to different sizes of Ag NPs

To examine the growth curves of bacterial cells exposed to Ag NPs, LB broth with Ag NPs (0, 2 μg/ml) was used, and the bacterial cell concentration was adjusted to 10^7 CFU/ml. Each culture was incubated in a shaking incubator at 37 °C for 24 h. Growth curves of bacterial cell cultures were attained through repeated measures of the optical density (O.D.) at 600 nm by using Synergy HTX microplate reader (Biotek) plate reader.

3. Results and discussion

The goal of this study was to develop a noninvasive, label-free whole-cell based capacitive biochip to test Ag NPs' toxicity. This aim was accomplished by probing responses of cells as biological reporters under the applied AC electrical frequency. For this, gold interdigitated microelectrodes based capacitor were patterned on SiO_2 surface by photolithograpy technique. *E. coli* cells were covalently coupled on sensor platform (Scheme 1). The electrical response of immobilized *E. coli* cells with and without exposure of NPs on capacitor surfaces was captured based on the change in dielectric properties, conductivity or charge distribution. The response of capacitive chips was further validated through FTIR and growth curves of bacterial cells exposed to different sizes of Ag NPs.

3.1. Characterization of Ag NPs by TEM and DLS

The three different sizes of Ag NPs used in this study were characterized using TEM analysis. The average sizes of NPs were found to be 10, 20 and 100 nm, respectively in TEM images as shown in Fig. 1a–c. The TEM images showed that the NPs were spherical and monodispersed in their distribution patterns that facilitated defined nano-sizes of Ag NPs to study their impact on exposure to *E. coli* cells-on-chip.

The particle sizes of Ag NPs used in this study was determined using dynamic light scattering measurement technique. In this technique, the hydrodynamic radius of the NPs was measured based on the principle of Brownian motion. The size distributions of the used NPs were depicted in Fig. 1d–f. As seen in case of 10 nm NPs, the particles were not seen monodispersed, but the average hydrodynamic radius of NPs was found to be around 16 nm (Fig. 1d). The estimated size in the DLS technique is based on the hydrodynamic diameter of the theoretical sphere that diffuses with identical size of particles and therefore, the measured size could be influential due to electrical double layer moving along with the particle. Thus, the measured size of 10 nm of NPs by TEM found differs than its measured hydrodynamic radius by DLS. The hydrodynamic radiuses for other two sizes of NPs were found to be around 20 and 100 nm (Fig. 1e and f), respectively.

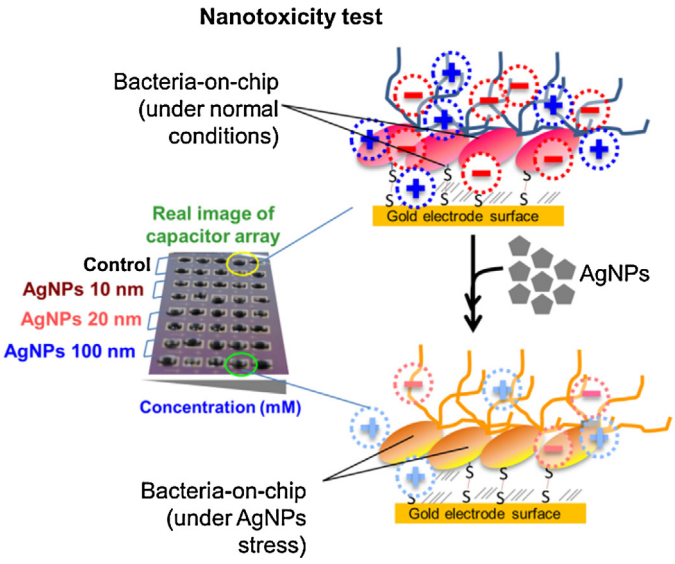

Scheme 1. Schematic of CoCT platform for probing toxicity of NPs.

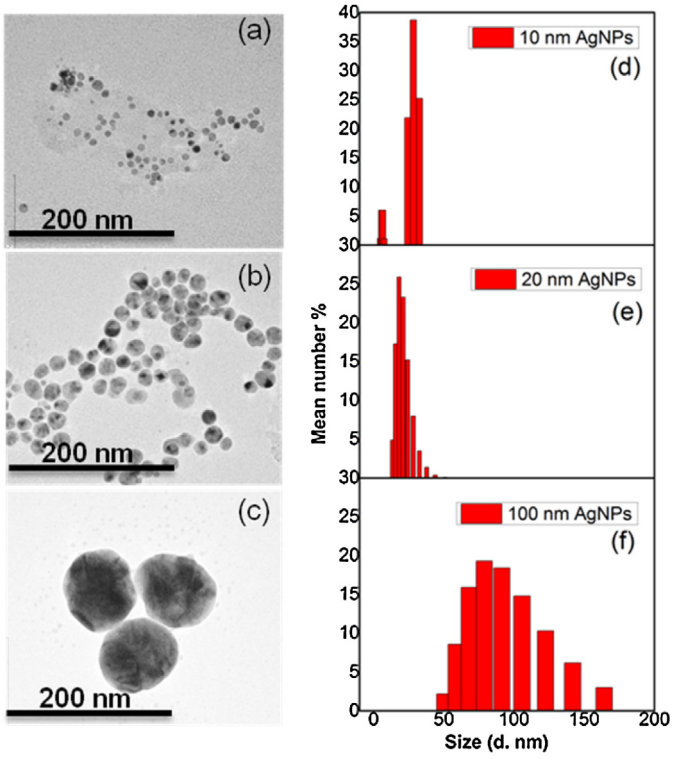

Fig. 1. (a-c) TEM images and (d–f) DLS size distribution of 5, 20 and 100 nm sizes of Ag NPs.

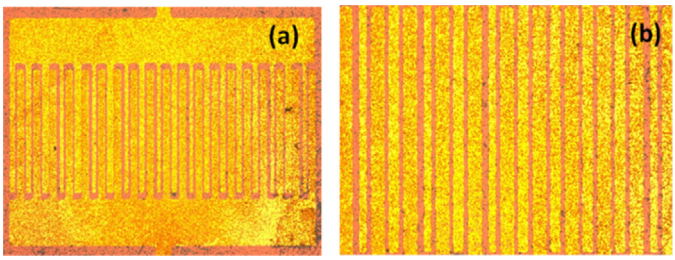

Fig. 2. Optical microscopic images of *E. coli* cells immobilized on; (a) capacitor chip at 5× and (b) a magnified portion of interdigitated electrodes of capacitor chip at 10× magnification.

3.2. *Optical micrographs of* E. coli *immobilized chip*

The optical images of *E. coli* cells immobilized on capacitor chip are shown in Fig. 2a and b. The optical microscopic images clearly indicated the density and distribution of cells indicating the dense immobilization of cells on electrodes of chip which is most suitable for probing NPs' toxicity in living *E. coli* cells-on-chip.

3.3. *Capacitance response of whole-cell based biosensor chip after exposure of Ag NPs*

The capacitance responses of whole-cell chip after exposure of Ag NPs were measured as a function of AC frequency (150–300 MHz). The capacitive response of Ag NPs on whole-cell biochip with three different sizes 10, 20 and 100 nm was shown in Fig. 3a–c, respectively. The cellular responses obtained through the whole-cell chip exhibited size dependent toxicity of silver NPs. It was observed that the capacitive response decreased with smaller size of Ag NPs (10 nm), which is attributed to the change in the potential of cell membrane upon the NPs's interaction with cells at the interface of the microelectrodes (Fig. 3a). However, the sensor response with larger 100 nm size of Ag NPs did not impose significant damage to the living cells-on-chip when compared with the control (no NPs, only cells-on-chip) (Fig. 3c). These results suggested that *E. coli* cells were sensitive to smaller NP sizes and severely affected by 10 nm NP sizes as evidenced by the dramatic loss of capacitance responses probably due to damage or collapse of living cell structure on sensor. This type of response was not seen with *E. coli* cells exposed with larger 100 nm sizes of Ag NPs which was probably because of their ability to resist against the larger sized Ag NPs (Fig. 4a and b). Fig. 4b shows the relative change in chip response of control (only cells), tests upon exposure of 10, 20 and 100 nm sizes of Ag NPs at 200 MHz applied AC frequency. The chip response against the heat-killed cells consistently showed significant drop in relative capacitance. This result suggested the inability of heat-killed cells to respond, which is an indication that the sensor response is attributed to the living activity of cells. This type of signal was correlated to the impact of NPs imposed on the living cells. It is clear from Fig. 4b that after heat-killing cells, the relative capacitive response dramatically dropped to a maximum extent and a similar response were also seen with normal cells exposed to 10–20 nm Ag NPs. This result can be compared to the sensor response obtained with heat-killed cells that show similar responses and suggest the smaller Ag NPs are lethal to cells.The capacitive response of chip upon exposure of 10–20 nm size at 0.2–0.8 μg/ml concentration was found to decline

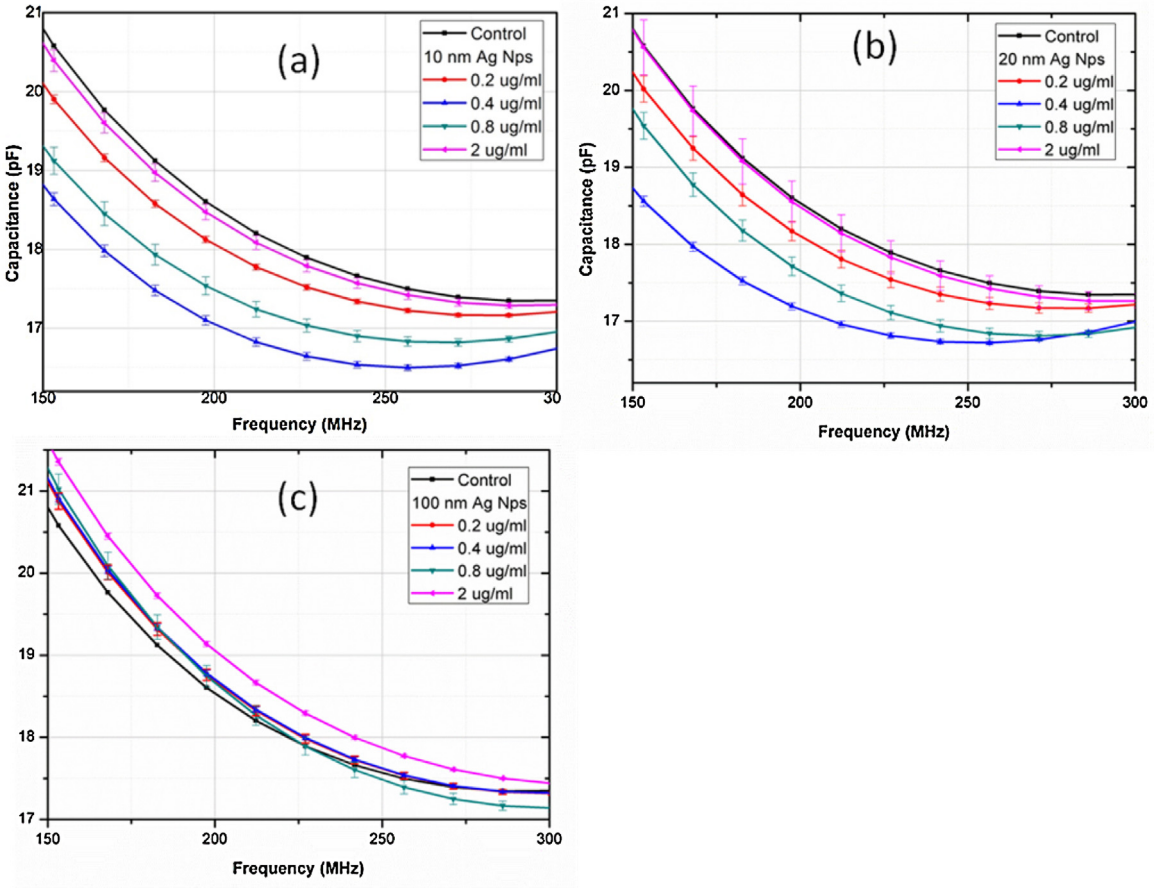

Fig. 3. Change in capacitance from whole-cell chip as a function of applied frequency (100–300 MHz) when exposed to different concentration (0.2–2 μg/ml) of (a) 10 nm (b) 20 nm and (c) 100 nm size of Ag NPs.

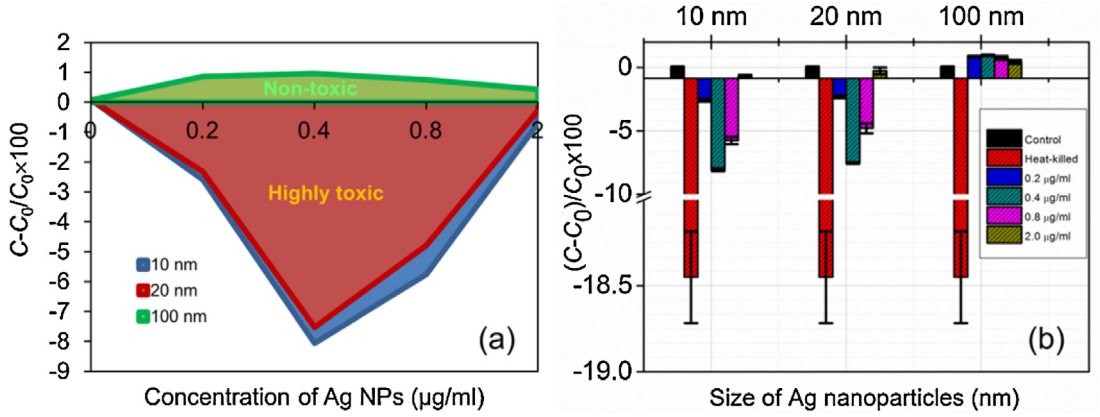

Fig. 4. a Relative change in capacitance responses at 200 MHz from whole-cell chip against three different sizes such as 10, 20 and 100 nm of Ag NPs at various concentrations ranging from 0.2–2 μg/ml on sensor chip. Areas under the curves are filled to distinguish effects on different sizes of Ag NPs based on the extent of toxicity effects. Fig. 4b shows bar graph of along with heat-killed cell (HKC) responses.

significantly (Fig. 4a). The results suggest that the increase in concentration of NPs (ranging 0.2–0.8 μg/ml) also affected the cells that increased the severely of cellular toxicity of NPs. Such effects normally occur due to accumulation of NPs or transport activity of NPs across the cell membrane, and this combined with impaired cell membrane function making the reduced cell's growth potential [15,26]. The interaction of bacterial cells with NPs probably yielded a reduction of net surface charges and this may have resulted in a decrease in relative change in capacitance response. However, relative capacitive response with exposure of 100 nm sizes of NPs did not show a considerably lethal effect which was closer to control responses. This result suggested that the cells did not affected severely by the 100 nm size of Ag NPs compared to smaller size (10–20 nm).

3.4. FTIR spectra of whole-cell based biosensor chip after exposure of Ag NPs

E. coli's outer wall is composed of an asymmetric lipid bilayer. The inner leaflet is mainly composed of L-aphosphatidylethanolamine (PE) and the outer leaflet is composed of lipopolysaccharide (LPS) biomolecules [27]. The ATR-FTIR peaks of an *E. coli* before exposure of Ag NPs were assigned to bands at 1634 cm^{-1}(amide I) arising principally from ν(C═O) stretching vibrations; bands at 1554 cm^{-1} (amide II) due primarily to N—H bending with contributions from the C—N stretching vibrations of the peptide group as shown in Fig. 5. The bands around 1280–1200 cm^{-1} arise from the nucleic acid bands overlapping with the asymmetric stretching mode υ_a of the phospholipid phospho-diester (PO_2^-) and non-stoichiometric lipopolysaccharides PO_2^- (LPS). The peaks between 1200 and 950 cm^{-1} are due to the vibrations of the sugar rings of LPS and also with the sugar rings from other cell moieties, such as peptidoglycan and exopolysaccharides (EPS) or capsular polysaccharides (CPS) [28].

The changes in the FTIR spectra for the *E. coli* cells treated with 10, and 100 nm Ag NPs is shown in Fig. 5. The intensity of the spectra was found to decrease with smaller size of Ag NPs. LPS spectra contain a relatively broad peak in the carbohydrate (O-antigen) region [ν(CO, COC); 1055 cm^{-1}, 1168 cm^{-1}] in *E. coli* spectra. When 100 nm Ag NPs interacted, LPS peak 1055 and 1168 cm^{-1} were shifted to lower wavenumber of 1045 and 1159 cm^{-1}, respectively. However, these peaks disappeared with cells treated with 10 nm size of NPs. This was probably due to the weakening of C—O, C—C, and POH bond caused by an increase in the degree or strength of hydrogen bonding with NPs [27]. The above results showed that the outer membrane of *E. coli* was indeed damaged, which was triggered by

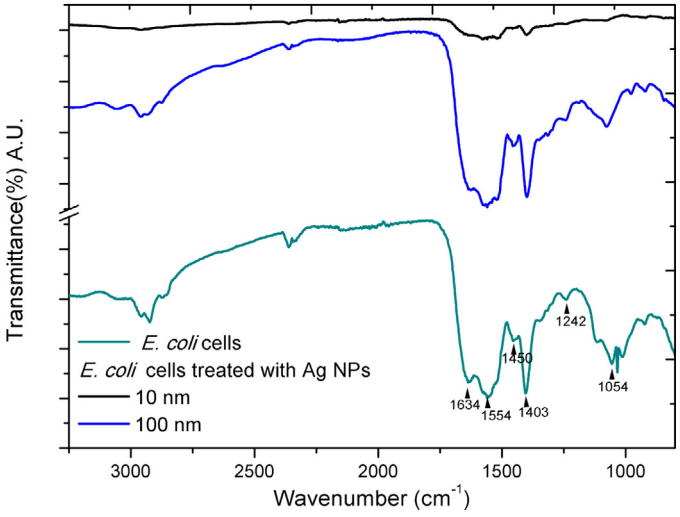

Fig. 5. FTIR spectra of *E. coli* cells-on-chip treated before and after exposure of Ag NPs with different sizes.

the toxic nature of smaller 10 nm sized Ag NPs. These results are in accordance with capacitive chip response results when different sizes of Ag NPs exposed to *E. coli* cells.

3.5. Growth curves of E. coli cells exposed to different sizes of Ag NPs

Growth of *E. coli* cells exposed to different sizes of Ag NPs was conducted to validate the *E. coli* CoCT response and all the toxicity parameter such as sizes (0, 10, 20 and 100 nm) and maximum concentration (2 μg/ml) of Ag NPs were kept same as in *E. coli* CoCT experiment.

The growth curves of bacterial cells treated with different sizes of Ag NPs indicated that Ag NPs could inhibit the growth of bacterial cells. The growth curves of Ag NPs treated *E. coli* cells are shown in Fig. 6. The bacterial growths of cells treated with 10 and 20 nm Ag-NPs were inhibited in comparision with 100 nm. The bacterial growth of the cells treated with 100 nm of Ag-NPs was also slightly lower than that of cells in the control group. The above result indicated that reactive oxygen species may be formed by lower size of Ag NPs inhibit in cellular respiration. As a result, lower size of Ag NPs cause inhibition of bacterial growth and reproduction, which is in good agreement with a previous study, which showed that the respiratory chain activity in *E. coli* was inhibited by Ag

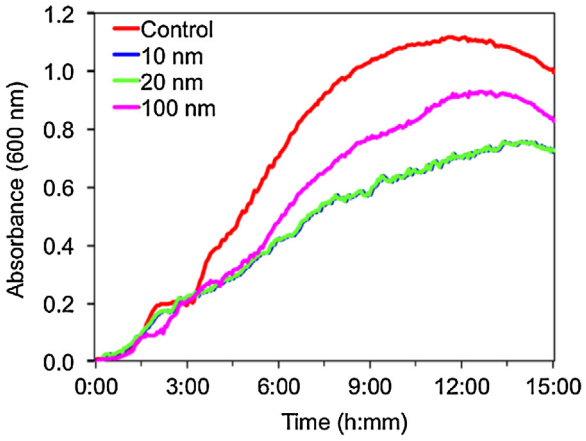

Fig. 6. Growth curves of *E. coli* cells treated before and after exposure of Ag NPs with different sizes.

NPs [29] and also in accordance with our *E. coli* CoCT results in Figs. 3–4. However, the correct mechanism of action of Ag NPs on bacteria is still unknown. The possible mechanism involves the NPs get attached to the cell membrane and their interaction leading to break the inner membrane and that could possibly inactivate respiratoty chain dehydrogenases [18,30]. The size of the nanoparticle implies its surface area to come in contact with the surface of bacterial cells. The larger of the size of Ag NPs, the lesser the surface area come in contact to the cell surface, thefore the lesser interaction with bacteria and lead to higher growth of cells as shown in Fig. 6 with 100 nm of Ag NPs.

4. Conclusions

In this study, capacitor arrays immobilized with *E. coli* cells were employed as a whole-cell biosensor chip to probe the cytotoxicity of Ag NPs. Here, *E. coli* cells were utilized as biological reporters and probed for electrical behavior of cells when interacted with Ag NPs using nFEIS. Our results suggested that *E. coli* cells were sensitively and severely affected by smaller 10 nm sizes of NPs, because cells exhibited dramatic loss of capacitance responses mainly because of the severe cellular damage. Contrastingly, *E. coli* cells were not severely affected with the larger 100 nm size of Ag NPs which was probably because cells-on-chip were capable of resisting to perturbations induced larger NP sizes. Further, the whole-cell-chip responses were also validated by FTIR analysis and growth of cell/cellular debris before and after the NPs exposure. The biosensor developed in this study can potentially be applied for the rapid detection of nanomaterias and chemicals that induce cytotoxicity in food, pharmaceutical preparations and environmental samples.

Acknowledgements

This work was supported by the Scientific and Technological Research Council of Turkey (TUBITAK), Grant no: 112E051. We thank Turgay Gönül for TEM imaging of samples.

References

[1] R.N. Seetharam, K.R. Sridhar, Nanotoxicity: threat posed by nanoparticles, Curr. Sci. 93 (2007) 769–770.
[2] L. Mazzola, Commercializing nanotechnology, Nat. Biotechnol. 21 (2003) 1137–1143.
[3] P.H. Hoet, I. Bruske-Hohlfeld, O.V. Salata, Nanoparticles—known and unknown health risks, J. Nanobiotechnol. 2 (2004) 12.
[4] A. Nel, T. Xia, L. Madler, N. Li, Toxic potential of materials at the nanolevel, Science 311 (2006) 622–627.
[5] A. Ivask, A. Elbadawy, C. Kaweeteerawat, D. Boren, H. Fischer, Z. Ji, et al., Toxicity mechanisms in *Escherichia coli* vary for silver nanoparticles and differ from ionic silver, ACS Nano 8 (2014) 374–386.
[6] B. Nowack, H.F. Krug, M. Height, 120 years of nanosilver history: implications for policy makers, Environ. Sci. Technol. 45 (2011) 1177–1183.
[7] C. Marambio-Jones, E.M.V. Hoek, A review of the antibacterial effects of silver nanomaterials and potential implications for human health and the environment, J. Nanopart. Res. 12 (2010) 1531–1551.
[8] T.M. Tolaymat, A.M. El Badawy, A. Genaidy, K.G. Scheckel, T.P. Luxton, M. Suidan, An evidence-based environmental perspective of manufactured silver nanoparticle in syntheses and applications: a systematic review and critical appraisal of peer-reviewed scientific papers, Sci. Total Environ. 408 (2010) 999–1006.
[9] B.P. Colman, C.L. Arnaout, S. Anciaux, C.K. Gunsch, M.F. Hochella, B. Kim, et al., Low concentrations of silver nanoparticles in biosolids cause adverse ecosystem responses under realistic field scenario, PLoS One 8 (2013) e57189.
[10] G. Oberdorster, E. Oberdorster, J. Oberdorster, Nanotoxicology: an emerging discipline evolving from studies of ultrafine particles, Environ. Health Perspect. 113 (2005) 823–839.
[11] S. Chatterjee, A. Bandyopadhyay, K. Sarkar, Effect of iron oxide and gold nanoparticles on bacterial growth leading towards biological application, J. Nanobiotechnol. 9 (2011) 34–37.
[12] A. Ivask, I. Kurvet, K. Kasemets, I. Blinova, V. Aruoja, S. Suppi, et al., Size-dependent toxicity of silver nanoparticles to bacteria, yeast, algae, crustaceans and mammalian cells in vitro, PLoS One 9 (2014) e102108.
[13] L. Brunet, D.Y. Lyon, E.M. Hotze, P.J. Alvarez, M.R. Wiesner, Comparative photoactivity and antibacterial properties of C60 fullerenes and titanium dioxide nanoparticles, Environ. Sci. Technol. 43 (2009) 4355–4360.
[14] O. Choi, Z. Hu, Size dependent and reactive oxygen species related nanosilver toxicity to nitrifying bacteria, Environ. Sci. Technol. 42 (2008) 4583–4588.
[15] K.K. Awasthi, A. Awasthi, N. Kumar, P. Roy, K. Awasthi, P.J. John, Silver nanoparticle induced cytotoxicity, oxidative stress, and DNA damage in CHO cells, J. Nanopart. Res. 15 (2013) 1898–1905.
[16] Y.P. Xie, Y.P. He, P.L. Irwin, T. Jin, X.M. Shi, Antibacterial activity and mechanism of action of zinc oxide nanoparticles against *Campylobacter jejuni*, Appl. Environ. Microbiol. 77 (2011) 2325–2331.
[17] J.S. Mcquillan, A.M. Shaw, Whole-cell *Escherichia coli*-based bio-sensor assay for dual zinc oxide nanoparticle toxicity mechanisms, Biosens. Bioelectron. 51 (2014) 274–279.
[18] Z. Lu, K. Rong, J. Li, H. Yang, R. Chen, Size-dependent antibacterial activities of silver nanoparticles against oral anaerobic pathogenic bacteria, J. Mater. Sci. Mater. Med. 24 (2013) 1465–1471.
[19] S.M. Hussain, K.L. Hess, J.M. Gearhart, K.T. Geiss, J.J. Schlager, In vitro toxicity of nanoparticles in BRL 3A rat liver cells, Toxicol. In Vitro 19 (2005) 975–983.
[20] G. Velve-Casquillas, M. Le Berre, M. Piel, P.T. Tran, Microfluidic tools for cell biological research, Nano Today 5 (2010) 28–47.
[21] D. Kim, Y.-S. Lin, C.L. Haynes, On-Chip evaluation of shear stress effect on cytotoxicity of mesoporous silica nanoparticles, Anal. Chem. 83 (2011) 8377–8382.
[22] E. Hondroulis, C. Liu, C.Z. Li, Whole cell based electrical impedance sensing approach for a rapid nanotoxicity assay, Nanotechnology 21 (2010) 315103–315114.
[23] F.A. Alexander Jr., E.G. Huey, D.T. Price, S. Bhansali, Real-time impedance analysis of silica nanowire toxicity on epithelial breast cancer cells, Analyst 137 (2012) 5823–5828.
[24] A. Qureshi, A. Pandey, R.S. Chouhan, Y. Gurbuz, J.H. Niazi, Whole-cell based label-free capacitive biosensor for rapid nanosize-dependent toxicity detection, Biosens. Bioelectron. 67 (2015) 100–106.
[25] E.A. de Vasconcelos, N.G. Peres, C.O. Pereira, V.L. da Silva, E.F. da Silva, Jr., R.F. Dutra, Potential of a simplified measurement scheme and device structure for a low cost label-free point-of-care capacitive biosensor, Biosens. Bioelectron. 25 (2009) 870–876.
[26] T. Warnecke, R.T. Gill, Organic acid toxicity, tolerance, and production in *Escherichia coli* biorefining applications, Microb. Cell Fact. 4 (2005) 25–33.
[27] M.A. Ansari, H.M. Khan, A.A. Khan, M.K. Ahmad, A.A. Mahdi, R. Pal, et al., Interaction of silver nanoparticles with *Escherichia coli* and their cell envelope biomolecules, J. Basic Microbiol. 54 (2014) 905–915.
[28] W. Bouhedja, G.D. Sockalingum, P. Pina, P. Allouch, C. Bloy, R. Labia, et al., ATR-FTIR spectroscopic investigation of *E. coli* transconjugants beta-lactams-resistance phenotype, FEBS Lett. 412 (1997) 39–42.
[29] W.R. Li, X.B. Xie, Q.S. Shi, H.Y. Zeng, Y.S. Ou-Yang, Y.B. Chen, Antibacterial activity and mechanism of silver nanoparticles on *Escherichia coli*, Appl. Microbiol. Biotechnol. 85 (2010) 1115–1122.
[30] M. Rai, A. Yadav, A. Gade, Silver nanoparticles as a new generation of antimicrobials, Biotechnol. Adv. 27 (2009) 76–83.

Biographies

Dr. Javed H. Niazi received his Ph.D. degree in Biochemistry in 2003 from Gulbarga University, India. He worked as postdoctoral fellow and later visiting scientist from 2004 to 2006 at Gwangju Institute of Science & Technology and Korea Institute of Science & Technology, South Korea. Later he continued his research as a postdoctoral researcher turned Research Professor at School of Life Sciences and Biotechnology, Korea University, South Korea during 2007–2009. He joined Faculty of Engineering

& Natural Sciences at Sabanci University as a visiting faculty, and currently working as Senior Researcher at Sabanci University Nanotechnology Research & Application Center (SUNUM), Turkey. His research areas include: (a) in vitro selection and modification of synthetic ssDNA/RNA aptamers as affinity ligands for disease biomarkers and drugs; (b) aptamer-facilitated biomarker discovery; (c) design and development of novel assays for biosensor applications-mainly for cardiovascular and cancer diseases and (d) nanotoxicology.

Ashish Pandey recieved his master degree in nanotechnology from MS University of Baroda, India. He is currently doing Ph.D. in material science and engineering programme at Sabanci University, Istanbul, Turkey.

Prof. Yasar Gurbuz received his B.Sc. degree in electronics engineering in 1990 from Erciyes University in Turkey, M.Sc. degree in 1993 and Ph.D. degree in 1997 in electrical engineering from Vanderbilt University in the USA. He worked as a senior research associate at Vanderbilt between 1997 and 1999. From 1999 to 2000 he worked at Aselsan Inc. He joined Sabanci University in 2000 as a faculty member in the Faculty of Engineering and Natural Sciences, where he is currently a full professor. His research areas include RF/Analog/Mixed-Signal Integrated Circuits, solid-state devices and sensors, and microelectromechanical systems (MEMS). He is a member of IEEE and SPIE.

Dr. Volkan Ozguz received his Ph.D. degree in Electrical Engineering from North Carolina State University, Raleigh, North Carolina in 1986. He was Fulbright and NATO Fellow during graduate studies. From 1986 to 1987, he was a visiting assistant professor at North Carolina State University and scientist at Microelectronic Center of North Carolina. From 1987 to 1989, he was the manager of the Advanced Processes Dept. at TELETAS-Alcatel. From 1989 to 1995, he was a research faculty at the University of California at San Diego. He joined Irvine Sensors Corporation in 1995–2009 where he was the Chief Technology Officer. Since 2010, he is the director of Sabanci Univeristy Nanotechnology Reserach and Applciation Center (SUNUM).

Dr. Anjum Qureshi received her Ph.D. degree in Physics in 2008 from MS University of Baroda, India. She is currently working as a research faculty at Sabanci University Nanotechnology Research & Application Center, Turkey. Her research interests include studying physics of biological systems, detection of cardiac/cancer diseases biomarkers by electrochemical biosensors and modification of polymer nano-composites and nanomaterials by irradiation.